



Since January 2020 Elsevier has created a COVID-19 resource centre with free information in English and Mandarin on the novel coronavirus COVID-19. The COVID-19 resource centre is hosted on Elsevier Connect, the company's public news and information website.

Elsevier hereby grants permission to make all its COVID-19-related research that is available on the COVID-19 resource centre - including this research content - immediately available in PubMed Central and other publicly funded repositories, such as the WHO COVID database with rights for unrestricted research re-use and analyses in any form or by any means with acknowledgement of the original source. These permissions are granted for free by Elsevier for as long as the COVID-19 resource centre remains active.

● *Original Contribution*

## USE OF LUNG ULTRASOUND TO DIFFERENTIATE CORONAVIRUS DISEASE 2019 (COVID-19) PNEUMONIA FROM COMMUNITY-ACQUIRED PNEUMONIA

GUOLIANG TAN,<sup>\*,†,2</sup> XIHUA LIAN,<sup>‡,§,2</sup> ZHIXING ZHU,<sup>‡,¶</sup> ZHENHUA WANG,<sup>||</sup> FANG HUANG,<sup>#</sup> YING ZHANG,<sup>§</sup>  
YANPING ZHAO,<sup>§</sup> SHAOZNG HE,<sup>‡,§</sup> XIALI WANG,<sup>‡</sup> HAOLIN SHEN,<sup>\*\*</sup> and GUORONG LYU<sup>‡,§,\*\*,††,‡‡2</sup>

\* Department of Critical Care Medicine, Second Affiliated Hospital of Fujian Medical University, Fujian, China; † Department of Infectious Disease, Wuhan Jinyintan Hospital, Wuhan, China; ‡ Collaborative Innovation Center for Maternal and Infant Health Service Application Technology of Education Ministry, Quanzhou Medical College, Fujian, China; § Department of Ultrasound Medicine, Second Affiliated Hospital of Fujian Medical University, Fujian, China; ¶ Department of Respiratory and Critical Care Medicine, Second Affiliated Hospital of Fujian Medical University, Fujian, China; || Department of Cardiovascular Disease, Second Affiliated Hospital of Fujian Medical University, Fujian, China; # Department of Radiology, Second Affiliated Hospital of Fujian Medical University, Fujian, China; \*\* Department of Ultrasound Medicine, Zhangzhou Municipal Hospital, Fujian, China; †† Affiliated Hospital of Quanzhou Medical College, Quanzhou, China; and ‡‡ Jinjiang Municipal Hospital, Fujian, China

(Received 8 April 2020; revised 7 May 2020; in final form 8 May 2020)

**Abstract**—To investigate the feasibility of lung ultrasound in evaluating coronavirus disease 2019 (COVID-19) and distinguish the sonographic features between COVID-19 and community-acquired pneumonia (CAP), a total of 12 COVID-19 patients and 20 CAP patients were selected and underwent lung ultrasound. The modified Buda scoring system for interstitial lung disease was used to evaluate the severity and treatment effect of COVID-19 on ultrasonography. The differences between modified lung ultrasound (MLUS) score and high-resolution computed tomography (HRCT) Warrick score were analyzed to evaluate their correlation. COVID-19 showed the following sonographic features: thickening (12/12), blurred (9/12), discontinuous (6/12) pleural line; rocket sign (4/12), partially diffused B-line (12/12), completely diffused B-line (10/12), waterfall sign (4/12); C-line sign (5/12); pleural effusion (1/12) and pulmonary balloon (Am line, 1/12). The last two features were rarely seen. Differences of ultrasonic features, including lesion range, lung signs and pneumonia-related complications, between COVID-19 and CAP were statistically significant ( $p < 0.05$  or  $0.001$ ). MLUS scores ( $p = 0.006$ ) and HRCT Warrick scores ( $p = 0.015$ ) increased as the severity of COVID-19 increased. The differences between moderate (29.00 [25.75–37.50]) and severe (43.00 [38.75–47.25]) ( $p = 0.022$ ) or between moderate and critical (47.50 [44.25–50.00]) ( $p = 0.002$ ) type COVID-19 were statistically significant, compared with those between severe and critical types. Correlation between MLUS scores and HRCT Warrick scores was positive ( $r = 0.54$ ,  $p = 0.048$ ). MLUS scores ( $Z = 2.61$ ,  $p = 0.009$ ) and HRCT Warrick scores ( $Z = 2.63$ ,  $p = 0.009$ ) of five severe or critical COVID-19 patients significantly decreased as their conditions improved after treatment. The differences of sonographic features between COVID-19 and CAP patients were notable. The MLUS scoring system could be used to evaluate the severity and treatment effect of COVID-19. (E-mail: [lgr\\_feus@sina.com](mailto:lgr_feus@sina.com)) © 2020 Published by Elsevier Inc. on behalf of World Federation for Ultrasound in Medicine & Biology.

**Key words:** Coronavirus disease 2019, Ultrasound, Tomography, X-ray computed, Lung, Pneumonia.

### INTRODUCTION

Coronavirus disease 2019 (COVID-19) refers to a type of pneumonia infected by severe acute respiratory syndrome coronavirus 2 (SARS-CoV-2), which has swept the globe. COVID-19 is a newly identified category B infectious

disease based on the infectious disease classification system of the Chinese Center for Disease Control and Prevention, with the characteristics of infectivity, concealment and a long incubation period (Jin et al. 2020). COVID-19 is likely to occur in a dense crowd and may cause fatal infection (Li et al. 2020). Lethal COVID-19 is found more commonly in patients with underlying diseases such as hypertension, diabetes mellitus, cardiovascular diseases and respiratory diseases (The Novel Coronavirus Pneumonia Emergency Response Epidemiology Team, 2020). COVID-19 poses a

Address correspondence to: Guorong Lyu, MD; 18965525702; 2 Ji'an Road, Luojiang District, Quanzhou, China. E-mail: [lgr\\_feus@sina.com](mailto:lgr_feus@sina.com)

<sup>2</sup> Guoliang Tan, Xihua Lian and Guorong Lyu contributed equally to this work and should be considered co-first authors.

severe threat to human health. Early diagnosis and timely intervention are reported to reduce the incidence of severe cases of COVID-19 and prevent the progression of COVID-19 cases to critical condition (Jin et al. 2020).

Early clinical diagnosis of COVID-19 depended on the real-time fluorescence quantitative reverse transcription–polymerase chain reaction detection of virus nucleic acids and chest computed tomography (CT) scan (Jin et al. 2020). However, it is difficult to diagnose or follow up the geographically dispersed COVID-19 patients in critical condition by chest CT scan. Studies have demonstrated that point-of-care ultrasound (POCUS), which is portable, flexible and free of ionizing radiation, plays an important role in emergency and intensive care medicine (Volpicelli et al. 2012; Lichtenstein 2014) and can be applied for semi-quantitative assessment of the severity of pulmonary edema and interstitial lung disease (ILD) (Zeng et al. 2019a, 2019b; Zhu et al. 2020). However, it is imperative to find out how to semi-quantitatively diagnose COVID-19 in an early stage and make a differential diagnosis from other types of pneumonia (Tsung et al. 2012). The histologic changes in viral pneumonia are mainly characterized by interstitial lesions accompanied by lymphocyte infiltration and often pulmonary interstitial fibrosis in the advanced stage (Shen et al. 2003). Since ultrasound has been widely used in the diagnosis and differentiation of interstitial pulmonary abnormalities (Volpicelli et al. 2012; Lichtenstein 2014), we hypothesized that ultrasound could be used to differentiate COVID-19 from community-acquired pneumonia (CAP).

## MATERIALS AND METHODS

This clinical study protocol was reviewed and approved by the Institutional Review Board and the Ethics Committee of Quanzhou Medical College, Fujian, China (2019-10). Informed consent was obtained from every patient or their assignee for this research and to publish this paper, which is focused on their data and images.

### Clinical data

**COVID-19 patients.** A total of 12 confirmed COVID-19 patients were selected as participants, including four men and eight women ranging from 52–79 y old, with a median age of 60.5 y. All patients met the new diagnostic criteria for coronavirus pneumonia issued by the National Health Commission of the People's Republic of China. COVID-19 was divided into four clinical types: mild, moderate, severe and critical (Table 1) (Jin et al. 2020). Among the 12 cases, there were four patients with moderate type, four with severe type and four with critical type. All patients underwent chest CT examinations as part of the diagnosis. Four patients had underlying diseases, including one with

Table 1. Main clinical features of different types of COVID-19

Clinical Types	Main Clinical Features
Mild	Fever, dry cough, fatigue or other clinical symptoms; no imaging sign of pneumonia
Moderate	Fever, diarrhea or other respiratory tract symptoms; with imaging sign of pneumonia
Severe	Meet any of the following features: 1. Polypnea, respiratory rate (RR) $\geq 30$ times/min; 2. In the resting state, peripheral venous oxygen saturation $\leq 93\%$ ; 3. Partial pressure of oxygen in arterial blood/fractional percentage of inspired oxygen (PaO <sub>2</sub> /FiO <sub>2</sub> ) $\leq 300$ mm Hg (1 mm Hg = 0.133 kPa).
Critical	Meet any of the following features: Respiratory failure with mechanical ventilation; Shock; With other organ failure and need intensive care.

COVID-19 = coronavirus disease 2019; RR = respiratory rate.

hypertension, one with diabetes mellitus and two with cardiovascular diseases. After half a month of treatment, five patients improved from severe or critical type to moderate type (Table 2). The data were collected from Wuhan Jinyintan Hospital from January 20 to February 20, 2020.

**CAP patients.** A total of 20 confirmed CAP patients were enrolled as a control group, including eight men and 12 women, ranging from 48–76 y old, with a median age of 57.5 y. Inclusion criteria include: (i) patients who met the diagnostic criteria of CAP (Metlay et al. 2019; Reissig et al. 2012); (ii) patients who underwent chest ultrasound examinations; (iii) patients with clear pathogenic evidence or with relieved symptoms and disappeared abnormalities on ultrasound and CT images after antibiotics therapy. All CAP patients underwent COVID-19 nucleic acid testing with negative results. Among the 20 cases, 10 cases had clear pathogenic evidence (six with pneumococcal pneumonia, three with gram-negative pneumonia and one with mycoplasma pneumonia), five cases had pathologic proofs confirmed by lung biopsy, five cases were clinically diagnosed with relieved symptoms and disappeared abnormalities on ultrasound and CT images after antibiotics therapy and three cases had underlying diseases (hypertension, diabetes mellitus and cardiovascular disease, respectively). The data were collected from the Second Affiliated Hospital of Fujian Medical University, Zhangzhou Municipal Hospital, Jinjiang Municipal Hospital and the Affiliated Public Hospital of Quanzhou Medical College from December 2019 to February 2020.

### Lung ultrasound and chest CT examination

**Ultrasound instrument and examination.** Patients were examined by portable ultrasound diagnostic

Table 2. Clinical data of 5 COVID-19 patients who improved from severe or critical type to moderate type

Case number	Age (y)	Sex	Type and clinical features	Underlying diseases
Case 1	56	Female	Critical; respiratory failure, mechanical ventilation	Diabetes mellitus
Case 2	62	Male	Critical; acute renal failure, mechanical ventilation	Hypertension
Case 3	64	Female	Severe; polypnea, RR=36 times/min, peripheral venous oxygen saturation=90%	None
Case 4	72	Male	Severe; polypnea, oxygen inhalation, disease progression >50% in lung imaging	Cardiovascular disease
Case 5	70	Female	Severe; dyspnea, polypnea, impaired liver function	None

“Improve to moderate type” means that patients have no dyspnea and oxygen inhalation, and show normal liver and kidney functions.  
 COVID-19 = coronavirus disease 2019.

instruments in three versions: EDGE II (Sonosite, Bothell, Washington, USA) equipped with a 3.5–5 MHz convex array probe, s6 pro (SonoScape, Shenzhen, China) equipped with a 2–5 MHz convex array probe and Z6 (Mindray, Shenzhen, China) equipped with a 2–5 MHz convex array probe. Parameters and settings of imaging were optimized based on each individual scanning.

To meet clinical urgent requirements, bedside lung ultrasound in emergency (BLUE) protocol and BLUE-plus protocol were adopted for these patients to screen the lung at the upper BLUE-point, lower BLUE-point, phrenic point, posterolateral alveolar and/or pleural syndrome point (PLAPS-point) and posterior BLUE-point (Volpicelli *et al.* 2012). Thus, a total of 10 points were selected on both sides of the lung (Fig. 1). Images of pleural line, lung parenchyma and thoracic cavity at each point were recorded in each ultrasound section, along with 20 s of cine-loop. Lung ultrasound scanning was performed among CAP patients at the upper BLUE-point, lower BLUE-point, phrenic point, PLAPS-point and posterior BLUE-point, in addition to the lesion areas (Volpicelli *et al.* 2012; Lichtenstein 2014).

*Scoring system for lung ultrasound.* All patients were examined and evaluated by intensive care unit (ICU) physicians who had received ultrasound training and obtained qualifications, and if necessary, videos were recorded for remote consultation. The modified lung ultrasound (MLUS) scoring system used in this study was modified based on the ILD Buda scoring system (Buda *et al.* 2016) and high-resolution computed

tomography (HRCT) Warrick scoring system with a maximum score of 60 points (Table 3). The scoring system mainly consisted of three items: (i) pleural line involvement, including thickened, blurred, irregular or discontinuous pleural line; (ii) lung parenchymal involvement, including B-line, partially diffused B-line, completely diffused B-line (white lung) and lung consolidation; and (iii) complications, including pneumothorax, emphysema and pleural effusion. Pleural line, pulmonary parenchyma and complications were observed and scored respectively in each section. There were 10 sections of bilateral lungs, where the pleural line score was less than 18 points, the lung score was less than 34 points and the complication score was less than 8 points.

Table 3. Modified scoring system for interstitial pneumonia

Ultrasound signs	Scoring based on ultrasonic features in each section
<b>Pleural line (score ≤18 points)</b>	
Normal	0
Thickening (≥0.5 mm) or irregular	1
Blurred	2
Discontinuous, fragmented	3
<b>Pulmonary parenchyma (score ≤34 points)</b>	
No B line	0
B line ≤3	1
B line ≥4 or partially merged	2
B line fully integrated (white lung or waterfall sign)	3
Pulmonary consolidation or subpleural lesion	4
<b>Complications (score ≤8 points)</b>	
None	0
Am line (pulmonary balloon)	4
Pneumothorax and empyema	4
Pleural effusion	4

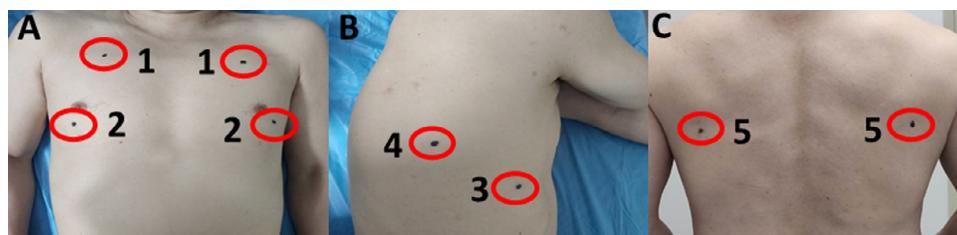


Fig. 1. Bedside lung ultrasound in emergency (BLUE)-plus protocol. (A) Upper blue point (1), lower blue point (2); (B) phrenic point (3); posterolateral alveolar and/or pleural syndrome point (PLAPS-point) (4); (C) posterior blue point (5).

Table 4. Semi-quantitative computed tomography scoring method in HRCT: Warrick et al

	Grading	Extent score segments involved		
		1–3	4–9	>9
HRCT abnormality	1	2	3	
Ground-glass opacities	1	2	3	4
Irregular pleural margin	2	3	4	5
Septal or subpleural lines	3	4	5	6
Honeycomb	4	5	6	7
Subpleural cyst	5	6	7	8

HRCT = high-resolution computed tomography.

**CT instruments and examination.** Chest CT was carried out for all patients in this study in accordance with the standard protocol with a 64-row multi-detector CT scanner (SOMATOM Perspective; Siemens, Germany). Scan ranged from the apex to the base of the lung with a HRCT scanning parameter of 120 HV, automatic mAs, 1.0 mm slice thickness, 0.90 pitch and field of view 30–40 cm. Lung window imaging was reconstructed with a high-frequency algorithm (width, 1600 Hu; level, –600 Hu).

**CT examination and scoring system.** Chest CT scan was performed for all patients. Warrick CT scoring criteria (Buda et al. 2016) was used to score the semi-quantitative chest CT scan in this study (Table 4). The CT results were evaluated by experienced CT imaging physicians in a blind fashion.

#### Statistical analysis

Continuous variables were expressed as medians (quartile 1–quartile 3), and categorical variables were expressed as counts and percentages. Wilcoxon rank sum tests for continuous variables and  $\chi^2$  or Fisher exact tests (where possible) for categorical variables were used to compare differences of test variables between the groups. Pearson correlation was applied to analyze the correlation between MLUS score and HRCT Warrick score. Probability values of <0.05 were considered statistically significant. All data analyses were performed with commercially available statistical analysis software packages (SSPS version 15.0; SSPS, Chicago, Illinois, USA).

## RESULTS

#### Sonographic features of COVID-19 and its differences with CAP

The main sonographic features of COVID-19 were as follows: (i) thickening (12/12), blurred and irregular (9/12) and fragmented pleural line (6/12) (Fig. 2); (ii) dispersed B-line and rocket sign (4/12), partially diffused B-line (12/12), completely diffused B-line for white lung (10/12) or waterfall sign (4/12) (Fig. 3), pulmonary

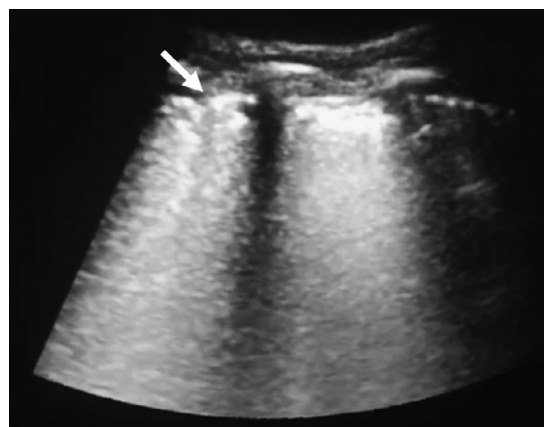


Fig. 2. Ultrasound image of a coronavirus disease 2019 (COVID-19) patient showing an abnormal fragmentary pleural line (arrow).

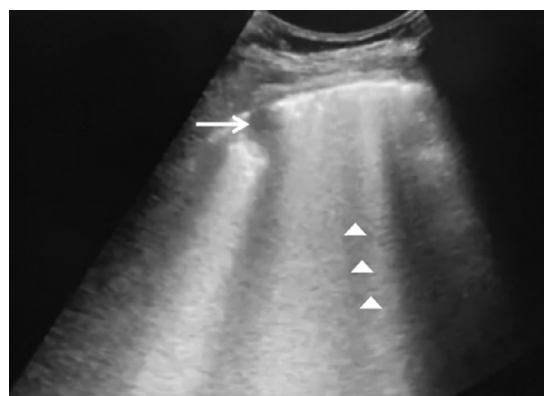


Fig. 3. Ultrasound image of a critical coronavirus disease 2019 (COVID-19) patient identifying a C-line sign (arrow) and diffused B line (arrowhead).

consolidations or subpleural focal lesions (5/12), generally less than 1.0 cm and shown as a C-line sign, were often seen among severe COVID-19 patients (Fig. 4), while large pulmonary consolidation was uncommon; and (iii) complications such as pleural effusion (1/12) and pulmonary balloon (Am line, 1/12) (Fig. 5) were rarely seen, while empyema and pneumothorax were not observed in our study. Differences in sonographic features between COVID-19 and CAP are shown in Table 5.

#### Correlation between MLUS scores and HRCT Warrick scores

A comparison of MLUS scores and HRCT Warrick scores among moderate, severe and critical groups is shown in Table 6. The mean values of MLUS scores and HRCT Warrick scores consistently and significantly increased as the severity of COVID-19 increased. MLUS scores were statistically significantly different between

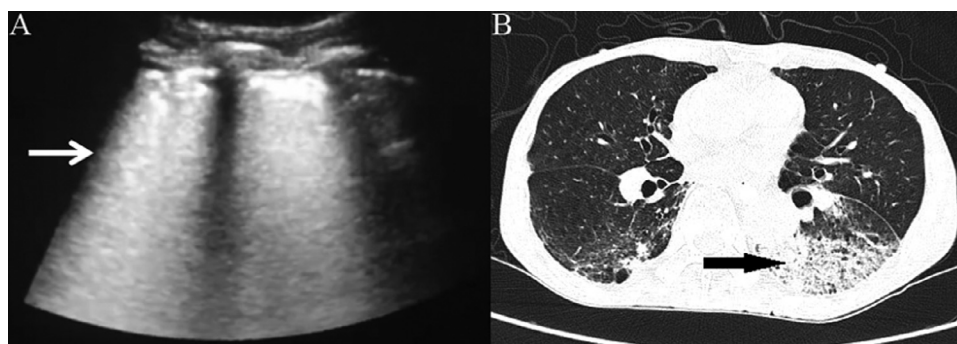


Fig. 4. Sonographic and computed tomography (CT) images of a patient with severe coronavirus disease 2019 (COVID-19) showing a diffusely B line (*arrow*) on ultrasound (A) and ground-glass opacity (*arrow*) on CT (B).

Table 5. The distinguishing sonographic features between COVID-19 pneumonia and CAP

	COVID-19 (12 cases)	CAP (20 cases)	$\chi^2$ value/ <i>p</i> value
<b>Lung lesions range</b>			
Lesions distributed $\leq 2$ lobes	0	19	24.16/ <i>p</i> < 0.001
Lesions distributed $\geq 3$ lobes or whole lungs	12	1	
<b>Pleural lesions range*</b>			
Lesions distributed $\leq 3$ ultrasound sections	0	15	15.0/ <i>p</i> < 0.001
Lesions distributed >3 ultrasound sections	10	5	
<b>Lung signs</b>			
B-line, rocket sign	4	10	27.12/ <i>p</i> < 0.001
Partially diffused B-line	12	4	
Completely diffused B-line (white lung)	10	4	
Waterfall sign	4	0	
Small consolidation or subpleural lesions (C-line sign)	5	2	
Large consolidation	0	19	
<b>Pneumonia-related complications</b>			
Pneumothorax	0	1	9.01/ <i>p</i> < 0.05
Pulmonary bullae or balloon (Am line)	1	0	
Empyema or pleural effusion	1	16	

\* Pleural lesions range were calculated by the 10 points of BLUE-plus protocol. BLUE = bedside lung ultrasound in emergency; CAP = community-acquired pneumonia; COVID-19 = coronavirus disease 2019.

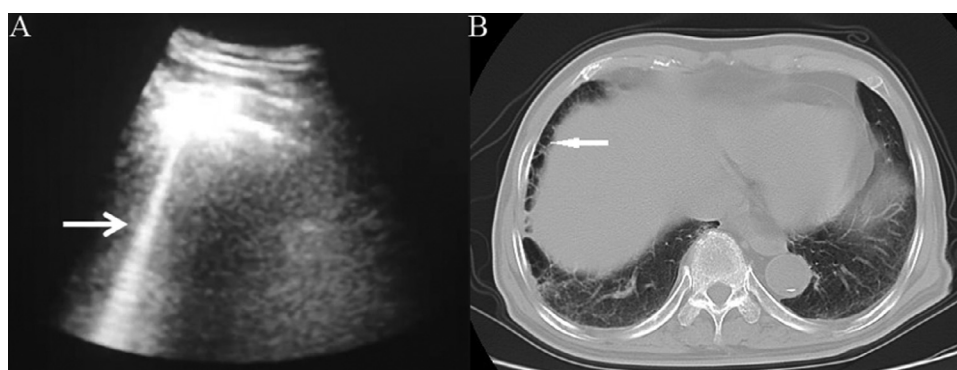


Fig. 5. Sonographic and computed tomography (CT) images of pulmonary cyst in a severe COVID-19 patient, showing an Am line (*arrow*) on ultrasound (A) and cyst (*arrow*) on CT (B).

the three groups ( $p = 0.006$ ), specifically between the moderate and severe groups ( $p = 0.022$ ) and the moderate and critical groups ( $p = 0.002$ ), but not between the severe and critical groups ( $p = 0.149$ ). The HRCT scores also showed statistically significant difference between the three groups ( $p = 0.015$ ), specifically

between the moderate and critical groups ( $p = 0.009$ ) and severe and critical groups ( $p = 0.014$ ), but not the moderate and severe groups ( $p = 0.783$ ). There was a positive correlation between the final results calculated by either MLUS scores or HRCT Warrick scores ( $r = 0.54$ ,  $p = 0.048$ ).

Table 6. The comparison of the points of modified ultrasound score and the points of HRCT Warrick score among the moderate, severe and critical groups

Group	MLUS scores	HRCT Warrick scores
Moderate group	29.00 (25.75–37.50)	16.00 (14.25–17.75)
Severe group	43.00 (38.75–47.25)*	16.50 (13.25–19.00)
Critical group	47.50 (44.25–50.00)*	21.00 (19.25–24.25)*,†

\*  $p < 0.05$  versus moderate group.

†  $p < 0.05$  versus severe group. HRCT = high-resolution computed tomography; MLUS = modified lung ultrasound.

#### Evaluation of follow-up

MLUS scores and HRCT Warrick scores of five severe or critical patients during follow-up are shown in Table 7.

## DISCUSSION

POCUS has found its wide application in emergency and critical care medicine (Volpicelli et al. 2012; Lichtenstein 2014). Many studies (Reissig et al. 2012; Volpicelli et al. 2012; Lichtenstein 2014; Alzahrani et al. 2017) have shown that ultrasound imaging is more sensitive than chest X-ray examination in the diagnosis of ventilator-associated pneumonia (Mongodi et al. 2016) and CAP (Ho et al. 2015). It can also make a sensitive diagnosis of viral pneumonia such as H1 N1 or H7 N9 earlier than chest X-ray examination (Testa et al. 2012; Ho et al. 2015) and thus has been recommended as an alternative screening method for such pneumonia in endemic areas (Testa et al. 2012; Tsai et al. 2014; Lissaman et al. 2019). However, ultrasound identification between viral pneumonia and bacterial pneumonia remains a huge challenge. This study indicated that ultrasound was feasible in the diagnosis of COVID-19, and the ultrasound images were mainly manifested as B-line artifact, rocket sign and partially or completely diffused B-line. Small consolidation and abnormal pleural line were detected in some cases. Noticeable differences in sonographic features were shown between COVID-19 and CAP. Ultrasound images of CAP were often manifested as large and circumscribed consolidation accompanied by bronchial gas phase or liquid phase, and pleural effusion was more common in CAP patients while their lung lesions were,

to some extent, limitedly distributed compared with those of COVID-19 patients. Consolidations were more extensive in bacterial pneumonia because a large number of fibrinogens permeated out from blood vessel to alveoli as the permeability of the blood vessel increased. Lung tissue was completely degassed and performed as a solid tissue echo in ultrasound, which was described as varying sizes of “hepatic-like changes.” Consolidations usually occurred in lung segment or sub-segment and might be accompanied by bronchial gas phase or liquid phase. Viral pneumonia such as severe acute respiratory syndrome (SARS) was histologically characterized by interstitial pneumonia with lymphocytes infiltration. The inflammation originated from bronchi and bronchioles, then pulmonary interstitial exudation, lymphedema and interstitial lung fibrosis emerged along the walls of bronchi, bronchiole and alveolus as well as the space among lobes. Consolidations can be detected in such areas in severe patients. Viral pneumonia could be easily distinguished from bacterial pneumonia by ultrasound with the pathologic differences. A limited number of studies (Tsung et al. 2012) showed that the pathologic features of COVID-19 were mainly manifested by diffused interstitial inflammation alveolar damage, including apoptosis and shedding of alveolar epithelial cells, formation of pulmonary hyaline membrane, obviously widened lobar space and infiltration of inflammatory cells composed of lymphocytes and monocytes. The similar pathologic features among COVID-19, SARS and Middle East Respiratory Syndrome (Shen et al. 2003; Xu et al. 2020) were the pathologic basis for the formation of lung ultrasound signs among patients with such diseases. The unique ultrasound signs of interstitial pneumonia included the disappearance of pleural line and the overlapping of B line, as well as white lung, waterfall sign and small consolidations in patients with severe interstitial pneumonia. Combined with other studies, this study indicated that different viral pneumonias had similar sonographic features, and there was still no evidence of obvious identification characteristics among them. However, compared with pulmonary edema and interstitial lung fibrosis, diffused B-line or even waterfall signs were more commonly detected in COVID-19 patients. The reasons might be that the more severe pulmonary inflammation and more abundant mucus were conducive to the

Table 7. The modified ultrasound score and HRCT Warrick score of the five severe or critical type patients during the treatment follow-up

Method	Before treatment	After treatment	Z value/p value
MLUS scores	41.00 (32.00~47.00)	18.00 (14.50~24.50)	2.61/p = 0.009
HRCT Warrick scores	17.00 (14.00~19.50)	9.00 (8.00~11.00)	2.63/p = 0.009

Five cases of severe or critical type improved to common type.

HRCT = high-resolution computed tomography; MLUS = modified lung ultrasound.

formation and fusion of B line in such patients (Volpicelli *et al.* 2012; Zeng *et al.* 2019a, 2019b; Zhu *et al.* 2020; Xu *et al.* 2020). Unexpectedly, large consolidation was rarely seen in COVID-19, and either bronchial fluid phase or gas phase was rarely seen in the consolidation, whereas nearly all the pleural abnormalities were detected in this study.

Many studies (Buda *et al.* 2016) indicated that lung ultrasound can be applied to the semi-quantitative evaluation of severity of pulmonary interstitial fibrosis. To meet the clinical needs of emergency and critical care ultrasound, BLUE-plus protocol was adopted to assess COVID-19 interstitial inflammation and fibrosis. Only 10 points (10 sections) were used for the observation of the pleural line, lung and thorax in the procedure, which significantly saved the evaluation time. Meanwhile, the Buda scoring system was modified (Table 1) by appropriately increasing the weight of pulmonary interstitial inflammation and the observation of acute complications, which was more suitable for the evaluation of severity of lung abnormalities of COVID-19 patients. The results showed that the scores of lung abnormalities, calculated by the modified Buda scoring system, increased as the severity of COVID-19 increased, and there was a moderate correlation between MLUS scores and Warrick scores that were calculated by the HRCT scoring method. Therefore, this new semi-quantitative pulmonary ultrasound assessment may be a viable approach for the evaluation of severity of interstitial pneumonia, including COVID-19. Furthermore, the study suggested that this new semi-quantitative method can also be used to evaluate the treatment effects of methods (such as CT) for COVID-19 during the follow-up. It is worth mentioning that this study also indicated that the MLUS scoring system is better in distinguishing the moderate group from the severe or critical group, compared with HRCT, which has an advantage in identifying the severe or critical group. This should be emphasized in the clinical application of the MLUS scoring system.

There are some limitations in this study. First, the sample size of this study was small. Second, mild COVID-19 patients were not included. Third, lung ultrasound was performed either in ICU or an isolated ward, and obtaining high-quality images was not allowed because of the emergent situations and poor-quality imaging system. More studies on prospective design are needed in the future.

## CONCLUSION

In summary, ultrasound imaging is a really effective choice for the evaluation of pulmonary abnormalities during the epidemic. Several different sonographic features between COVID-19 and CAP patients have been demonstrated in this study. MLUS scoring system is helpful for the evaluation of COVID-19 severity, while

POCUS plays a valuable role as an adjunct tool to HRCT in the assessment of COVID-19 patients.

*Conflict of interest disclosure*—The authors declare no competing interests.

*Acknowledgment*—This study was sponsored by the key Clinical Specialty Discipline Construction Program of Fujian, P.R.C [Grant (2017) 739], the Research Project of Science and Technology Department of Fujian Province, China (Grant 2018 J01288), the Youth Research Project of Health and Family Planning Commission of Fujian Province, China (Grants 2018-1-62 and 2018-2-23), the Quanzhou Science and Technology Project (Grants 2018 N012) and the Research Project of Collaborative Innovation Center for Maternal and Infant Health Service Application Technology (Grant XJM1802).

Medical writing guidance and recommendations for the study were provided by Professor Jibin Liu of Thomas Jefferson University, Philadelphia, PA, USA.

## REFERENCES

- Alzahrani SA, Al-Salamah MA, Al-Madani W, Elbarbary MA. Systematic review and meta-analysis for the use of ultrasound versus radiology in diagnosing of pneumonia. *Crit Ultrasound J* 2017;9:6.
- Buda N, Piskunowicz M, Porzezinska M, Kosiak W, Zdrojewski Z. Lung ultrasonography in the evaluation of interstitial lung disease in systemic connective tissue diseases: Criteria and severity of pulmonary fibrosis - analysis of 52 patients. *Ultraschall Med* 2016;37:379–385.
- Ho MC, Ker CR, Hsu JH, Wu JR, Dai ZK, Chen IC. Usefulness of lung ultrasound in the diagnosis of community-acquired pneumonia in children. *Pediatr Neonatol* 2015;56:40–45.
- Jin YH, Cai L, Cheng ZS, Cheng H, Deng T, Fan YP, Fang C, Huang D, Huang LQ, Huang Q, Han Y, Hu B, Hu F, Li BH, Li YR, Liang K, Lin LK, Luo LS, Ma J, Ma LL, Peng ZY, Pan YB, Pan ZY, Ren XQ, Sun HM, Wang Y, Wang YY, Weng H, Wei CJ, Wu DF, Xia J, Xiong Y, Xu HB, Yao XM, Yuan YF, Ye TS, Zhang XC, Zhang YW, Zhang YG, Zhang HM, Zhao Y, Zhao MJ, Zi H, Zeng XT, Wang YY, Wang XH. A rapid advice guideline for the diagnosis and treatment of 2019 novel coronavirus (2019-nCoV) infected pneumonia (standard version). *Mil Med Res* 2020;7:4.
- Li Q, Guan X, Wu P, Wang X, Zhou L, Tong Y, Ren R, Leung KSM, Lau EHY, Wong JY, Xing X, Xiang N, Wu Y, Li C, Chen Q, Li D, Liu T, Zhao J, Liu M, Tu W, Chen C, Jin L, Yang R, Wang Q, Zhou S, Wang R, Liu H, Luo Y, Liu Y, Shao G, Li H, Tao Z, Yang Y, Deng Z, Liu B, Ma Z, Zhang Y, Shi G, Lam TTY, Wu JT, Gao GF, Cowling BJ, Yang B, Leung GM, Feng Z. Early transmission dynamics in Wuhan, China, of novel coronavirus-infected pneumonia. *N Engl J Med* 2020;382:1199–1207.
- Lichtenstein DA. Lung ultrasound in the critically ill. *Ann Intensive Care* 2014;4:1.
- Lissaman C, Kanjanapoom P, Ong C, Tessaro M, Long E, O'Brien A. Prospective observational study of point-of-care ultrasound for diagnosing pneumonia. *Arch Dis Child* 2019;104:12–18.
- Metlay JP, Waterer GW, Long AC, Anzueto A, Brozek J, Crothers K, Cooley LA, Dean NC, Fine MJ, Flanders SA, Griffin MR, Metersky ML, Musher DM, Restrepo MI, Whitney CG. Diagnosis and treatment of adults with community-acquired pneumonia. An official clinical practice guideline of the American Thoracic Society and Infectious Diseases Society of America. *Am J Respir Crit Care Med* 2019;200:e45–e67.
- Mongodi S, Via G, Girard M, Rouquette I, Misset B, Braschi A, Mojoli F, Bouhemad B. Lung ultrasound for early diagnosis of ventilator-associated pneumonia. *Chest* 2016;149:969–980.
- Reissig A, Copetti R, Mathis G, Mempel C, Schuler A, Zechner P, Aliberti S, Neumann R, Kroegel C, Hoyer H. Lung ultrasound in the diagnosis and follow-up of community-acquired pneumonia: A prospective, multicenter, diagnostic accuracy study. *Chest* 2012;142:965–972.



- Shen MS, Yin T, Ji XL. Pathological diagnosis and differential diagnosis of severe acute respiratory syndrome. *J Clin Exp Pathol* 2003;19:387–389.
- Testa A, Soldati G, Copetti R, Giannuzzi R, Portale G, Gentiloni-Silveri N. Early recognition of the 2009 pandemic influenza A (H1 N1) pneumonia by chest ultrasound. *Crit Care* 2012;16:R30.
- The Novel Coronavirus Pneumonia Emergency Response Epidemiology Team. The epidemiological characteristics of an outbreak of 2019 novel coronavirus diseases (COVID-19) in China. *Chinese J Epidemiol* 2020;41:145–151.
- Tsai NW, Ngai CW, Mok KL, Tsung JW. Lung ultrasound imaging in avian influenza a (H7 N9) respiratory failure. *Crit Ultrasound J* 2014;6:6.
- Tsung JW, Kessler DO, Shah VP. Prospective application of clinician-performed lung ultrasonography during the 2009 H1 N1 influenza a pandemic: Distinguishing viral from bacterial pneumonia. *Crit Ultrasound J* 2012;4:16.
- Volpicelli G, Elbarbary M, Blaivas M, Lichtenstein DA, Mathis G, Kirkpatrick AW, Melniker L, Gargani L, Noble VE, Via G, Dean A, Tsung JW, Soldati G, Copetti R, Mouhammad B, Reissig A, Agricola E, Rouby JJ, Arbelot C, Liteplo A, Sargsyan A, Silva F, Hoppmann R, Breikreutz R, Seibel A, Neri L, Storti E, Petrovic T. International evidence-based recommendations for point-of-care lung ultrasound. *Intensive Care Med* 2012;38:577–591.
- Xu Z, Shi L, Wang Y, Zhang J, Huang L, Zhang C, Liu S, Zhao P, Liu H, Zhu L, Tai Y, Bai C, Gao T, Song J, Xia P, Dong J, Zhao J, Wang FS. Pathological findings of COVID-19 associated with acute respiratory distress syndrome. *Lancet Respir Med* 2020;8:420–422.
- Zeng LQ, Lyu GR, Li YY, Chen YJ, Li BY. In vitro experimental study for the formation mechanism of B line in lung ultrasound. *Chinese J Ultrasound Med* 2019;35:560–562.
- Zeng LQ, Lyu GR, Lian XH, Zhu ZX, Chen YJ, Xu ZR, Guo YN. Study on the correlation between B line in ultrasound and severity of pulmonary edema. *Chinese J Ultrasound Med* 2019;35:272–274.
- Zhu ZX, Lian XH, Zeng YM, Wu WJ, Xu ZR, Chen YJ, Li JY, Su XS, Zeng LQ, Lyu GR. Point-of-care ultrasound- A new option for early quantitative assessment of pulmonary edema. *Ultrasound Med Biol* 2020;46:1–10.